

We are IntechOpen, the world's leading publisher of Open Access books Built by scientists, for scientists

6,300

Open access books available

171,000

International authors and editors

190M

Downloads

Our authors are among the

154

Countries delivered to

TOP 1%

most cited scientists

12.2%

Contributors from top 500 universities



WEB OF SCIENCE™

Selection of our books indexed in the Book Citation Index
in Web of Science™ Core Collection (BKCI)

Interested in publishing with us?
Contact book.department@intechopen.com

Numbers displayed above are based on latest data collected.
For more information visit www.intechopen.com



Chapter

Climate Risks and Reasons for Concern along the Uruguayan Coast of the Río de la Plata Estuary

Gustavo J Nagy, José E Verocai, Leandro Capurro, Mónica Gómez-Erache, Ofelia Gutiérrez, Daniel Panario, Ernesto Brugnoli, Agustina Brum, Mario Bidegain and Isabel C. Olivares

Abstract

The Uruguayan coast of the Río de la Plata river estuary (RdLP) is 300 km long. It encompasses an inner tidal river and a middle and an outer estuary. The RdLP is a micro-tidal system dominated by river inflow from the Paraná and Uruguay rivers and southern winds with increasingly frequent wind-induced storm surges impacting the coast. The El Niño-Southern Oscillation influences the river inflow, prevailing winds, water/sea level and beach erosion. First, we focus on the IPCC Reasons for Concern (RFC) about the trends of climate risks threatening the Uruguayan coast. The trends and maxima of air temperature, water/sea levels and river inflow in three coastal stations from 1980 to 2019 show temporal changes attributable to climate change and El Niño-Southern Oscillation (ENSO). The occurrence, evolution and Monte Carlo simulations of return periods of the yearly river flow and sea level height maxima provide metrics of RFC to categorise the climate risks from past to projected future and the level of risk from undetectable to very high. Then, we summarise some current and expected climate risks and present the current adaptation framework and some expected impacts. The RFC has increased, reaching moderate to high-risk levels.

Keywords: ENSO, sea-level rise, extreme sea levels, river inflow, wind maxima, climate impacts, beach erosion, harmful blooms, Monte Carlo simulation

1. Introduction

1.1 Climate risks in the coastal and estuarine systems

Coastal systems are the first in line (exposed) to sea-level rise (SLR) and extreme weather events' adverse impacts, making them especially vulnerable and at risk [1, 2].

The number of published articles on climate change in marine environments has increased since 2000, reaching close to 4% on coastal and estuarine systems of all

climate change papers, <1% of which are on estuarine systems and their overlap with the other ones [3].

Indeed, estuaries are among the ecosystems that are most threatened by climate change, for example, acidification, SLR, storms and changes in rainfall [4–7]. In addition, they are subject to frequent perturbations, for example, from short-term tidal water level and salinity changes to long-term climatic changes due to the El Niño-Southern Oscillation (ENSO) and the North Atlantic Oscillations (NAO) and extreme events such as floods and storm surges [6, 8].

This chapter deals with the climate change, extreme weather, and climate risks along the Uruguayan coast (northern side) of the Rio de la Plata estuary (RdIP), which, due to its vast dimensions (300 km long and 40–230 km wide), openness to and exchange with the sea, littoral drift currents and morphodynamics, developed unique sandy beaches and dunes more typical of the shallow sea coastal systems [9, 10].

Furthermore, we analyse the IPCC concept of “Reasons for Concern” (RFC) [9], which addresses climate risk using five broad domains to assess the increased risk to societies and ecosystems; it synthesises how climate change risks accumulate with the global average temperature increase [10].

We explore the second Reason for Concern (RFC2) associated with extreme weather events and their risks to the coast from river and sea flooding to SLR.

Consequently, it is also essential to consider sea level variability because a change in the mean sea level (MSL) can disproportionately increase the likelihood that water levels will exceed the survival capacity of these socio-ecological systems.

1.2 Climate risks in the Rio de la Plata estuary (RdIP)

The (RdIP) (**Figure 1**) drains the waters of the La Plata basin (LPB) via the Paraná and Uruguay rivers, which flow through five countries (Argentina, Uruguay, Brazil, Paraguay and Bolivia) in the south-eastern region of South America, discharging freshwater into the estuary with low seasonality. However, it shows considerable inter-annual variability, mainly coinciding with the (ENSO) phases.

ENSO influences the LPB, with a strong correlation between the El Niño 3 and 3.4 Sea Surface Temperature (SST) index and precipitation, with a positive association between El Niño and increased rainfall [11–14]. The variability at inter-annual



Figure 1.

The Rio de la Plata estuary. Source: The Copernicus Sentinel-3 satellites on 14 February 2022 (<https://www.copernicus.eu/en/media/image-day-gallery/rio-de-la-plata-estuary>). CL (Colonia); Mvd (Montevideo); LdS (Laguna del Sauce); Ro (Rocha); BA: Buenos Aires; SB: Sandy beaches. The arrows show the drift transport of sediments.

timescales coincides with ENSO, while the decadal scales are related to equatorial SST gradients in the Atlantic and the Pacific [15]. The hydrologic cycle in LPB has a warm season (October–April) with an average rainfall of 5.5 mm/d and a cold season (May–September) with an average rainfall of less than two mm/d [16].

The RdIP shared by Argentina and Uruguay has been substantially affected by increased temperature, sea-level rise [17, 18], wind-regime changes, increased frequency and intensity of ENSO events and extreme weather and climate events like river floods, droughts and wind storms [19–22]. For example, changes in waves propagating from the E- and ESE-induced coastal erosion on the Argentinean coast [23, 24]. In the short term, ENSO-related variability influences erosion and accretion processes on the Uruguayan coast under strong La Niña (“LN”) and SW/SE winds and El Niño (“EN”) events and high SE winds, respectively. Besides, (“EN”) induces flooding of the Paraná and Uruguay rivers, significantly increasing the freshwater/sea level’s average height [25, 26].

However, there is scarce literature concerning the extremes, particularly the impacts on the northern coast, mainly related to severe and extreme wind-induced storm surges adversely impacting the sandy beaches, built environment and communities [17–19, 27]. Therefore, this chapter aims to present selected annual climatic averages and maxima during the recent past (focused on 1980–2019), posing risks to cultural and natural systems, such as the sandy beaches or stimulating cyanobacterial harmful algae blooms (Cyano-HABs) along the northern coast.

The research questions (RQs) focus on the Reasons for Concern (RFC 2) regarding the past, current and projected evolution of climatic variables and risks. For example, RQ 1: Is the increase in extreme weather events and their risks to the coast from river and sea flooding and sea-level rise (SLR) reaching high-risk levels? RQ 2: Are the extreme sea heights (ELS) increasing/decreasing or fluctuating over time? The study objectives are as follows:

1. Briefly review some relevant literature about climate risks along the RdIP northern coast.
2. Update the recent time series (1980–2019) of climatic, hydrological and SLR in the RdIP and its northern coast and describe the extreme events of these variables.
3. Discuss RFC2 along the northern coast, emphasising the sandy beaches and cyanobacterial harmful blooms (Cyano-HABs).
4. Summarise the status of the Uruguayan National Adaptation Plan-Coasts (C-NAP) framework, vulnerabilities and projected scenarios in the medium term (2050).

1.3 Approach of the study

The approach of this chapter is a mix of i) a narrative literature review and priorities for future research of climate risks and Reasons for Concern focused on the research question, ii) an update of relevant literature from the co-authors and iii) data analysis of primary data collection.

The chapter is structured as follows: Section 1 is the introduction, Section 2 summarises the study site and methods, emphasising the climate risks and the concept of Reasons for Concern (RFC). Section 3 presents the observed weather, hydroclimatic

and water–/sea-level trends, extreme flow and height levels and return periods focused on the current (1980–2019) time horizon. Section 4 discusses the Reasons for Concern. Section 5 summarises the current state of adaptation based on the National Adaptation Plan Coast, and finally, Section 6 deals with the summary and conclusion.

2. Methodology

2.1 Study site

The RdIP is a vast (38,000 km²) micro-tidal (amplitude: <0.5 m along the northern coast) runaway with a partially stratified system, that is to say, the stratification persists over several tidal cycles due to the micro-tidal amplitude [28]. The wind, river inflow and ENSO forcings control the stratification/mixing cycle and the estuarine front location on daily, seasonal and inter-annual timescales [26, 28, 29]. The estuary has an extensive and permanent connection to the sea and high susceptibility to atmospheric drivers because of its large size and shallow depth (**Table 1**). The RdIP flow governs the salinity and turbidity and has typical monthly to inter-annual variations from around 20,000 to 30,000 m³s⁻¹ [29, 31, 32].

The satellite image (**Figure 1**) shows the mixing of freshwater (brown) and seawater (blue) visible from space during a typical La Niña-related low river flow with the middle estuary displaced inwards. The brown, greenish and blue colours display the inner tidal river, middle estuary and outer estuary, respectively, with Montevideo in the middle. Mixing freshwater with seawater creates eddies and estuarine salinity and turbidity fronts, which move seaward and riverward due to increased/decreased river flow and offshore/onshore axial winds [20, 28, 29, 32].

Most of the beaches along the RdIP Uruguayan coast are unstable wave-dominated environments, where the drift transport of sediment flows opposite to the current of the estuary channel [33, 34]. Both non-climate and climate factors (ENSO, storm surges and river floods) influence erosion, accretion and retreat processes [19].

Morphological and hydrological Type [6, 28–30]	Dimensions [28, 30]	River inflow [22, 28, 29]	Salinity [6, 23, 28–30]	Tides and SLR [17, 18, 22, 28, 29]
River-influenced and tidal river funnel-shaped coastal plain estuary Partially stratified (prevailing) to highly stratified, (prevailing) along the Canal Oriental at >17 m.	Total surface: 38 x 10 ³ km ² Middle and Outer regions: ~22 x 10 ³ km ² Width: Head: 40 km; Middle ~100 km Outer: 120–230 km.	The total average Q _F is ≈ 25–27 x 10 ³ m. s ⁻¹ , varying from <20 to >30 x 10 ³ m ³ s ⁻¹ during dry/wet years linked with La Niña/ El Niño events.	0–33, with an average of 8–10 at Montevideo and 20–25 at Punta del Este.	0.2 to 0.5 m along the northern coast. Observed SLR (2016): 11–12 cm. Expected SLR by 2050: ≈0.3 m

Table 1. Geomorphological and hydrological features of the Rio de la Plata estuary.

A comprehensive definition of the RdLP, based on morpho-sedimentary and hydrodynamical criteria, is “The funnel-shaped Rio de la Plata is a coastal plain estuary with a river palaeo valley (called Canal Oriental) along the northern coast [9], which behaves as a conduit channel for water and particles to the Ocean [29]”.

2.2 Climate, river flow, weather and sea-level data

Variability and magnitude of ENSO were determined by the NOAA Ocean Niño Index (ONI) considering the monthly anomalies of ocean surface temperature (SST) in the Niño 3.4 region (1980–2019) from http://www.cpc.ncep.noaa.gov/products/analysis_monitoring/ensostuff/ensoyears.shtml.

We considered the daily flows (m^3/s) of the Uruguay River (Q_{UY}), the lower Paraná River branches Guazú (Q_{PG}) and Las Palmas rivers (Q_{PLP}) from 1980 to 2019, which together represent the Rio de la Plata inflow computed as $Q_{\text{PG}} + Q_{\text{PLP}} + Q_{\text{UY}}$, taken from the National Water Institute (Argentina, www.ina.gov.ar). The Q_{PG} flow has much more impact on the northern coast than the Q_{PLP} . Then, we classified the years according to the ONI index (https://origin.cpc.ncep.noaa.gov/products/analysis_monitoring/ensostuff/ONI_v5.php).

For precipitation data, we used the ERA5 (European Reanalysis V5; <https://www.ecmwf.int/en/forecasts/dataset/ecmwf-reanalysis-v5>) for the period 1980–2019 verified against in situ observations up to 2015. Quality-assured monthly updates of ERA5 (1959 to present) are published within three months in real time [35].

We recopiled the extreme monthly air temperatures from the weather station “Carrasco” (Montevideo) and the yearly averages (1980–2019) from N° 86,560 “Colonia” and N°86,565 “Rocha” stations from “Instituto Uruguayo de Meteorología” (Inumet) <https://www.inumet.gub.uy/>. Although Rocha is on the Atlantic Ocean coast (**Figure 1**; *ca.* 150 km Eastern boundary of RdLP), we included it as the eastern boundary to compare it with previous reports.

For wind data, we recopiled information for Colonia, Carrasco and N°86,586 “Laguna del Sauce” (Eastern boundary of the RdLP, close to Punta del Este), also from the Inumet surface network.

For water/sea level, we analysed three tide gauge stations located at Colonia (Inner estuary), Montevideo (middle estuary) and Punta del Este (outer estuary), covering 300 km of the coastline.

The specific criterion to define a wind-induced storm surge from the tide gauge measurements is: in the records measured as the difference in hourly cut levels of an increase of ≥ 30 centimetres, and exceeding the level of 200 centimetres above zero, in the port of Montevideo (taken as the pattern for the three stations).

The selection of the risk levels for each RFC related to the SLR was based on identifying the damage produced or estimated on the Uruguayan coast [22, 26].

2.3 Criteria to classify extreme meteorological events

We used the following criteria for extreme meteorological events [36] and wind-induced storm surges, as applied to the Uruguayan coast [22]:

1. *Rare events*: Those that have a low probability of occurrence.
2. *Extreme events*: Those with extreme values of meteorological variables such as precipitation (e.g., river floods) and wind (e.g., storm surges). Extreme is

defined as taking the maximum yearly values or exceeding the 100-year return value (a probability of 0.01 occurring in any particular year).

3. *High-impact (severe) events*: These can be either short-lived weather systems (e.g., severe storms) or longer-duration events such as prolonged heat waves and droughts.
4. *Acute extremes*: Those with a rapid onset follow a short but severe course like extra-tropical cyclones (“wind-storms”) and convective storms with extreme wind speed, precipitation or coastal floods that can lead to devastating wind and flood damage.

For instance, we classified the gusts of wind events as rare (70–89 km/hour), extreme (90–109 km/h), severe/high-impact (110–139 km/h) and acute (>140 km/h) and for extreme water/sea height as rare (200–249 cm), extreme (250–299 cm), high-impact (300–349 cm) and acute (>350 cm).

1. *Height 200 cm*. Port closed for sports and craft boats. Sandy beaches prism flooded.
2. *Height 250 cm*. The municipal storm drains of Montevideo stopped working. Flooding of Santa Lucía river wetlands (western Montevideo).
3. *Height 280 cm*. The port closed for all activities, with the risk of severe damage to coastal infrastructure. Erosion of sandy beaches and dunes.
4. *Height 300 cm*. Increased risks and damages to the infrastructure and beaches.
5. *Height 350 cm*. Severe damage to the population. Potentially irreversible impacts in some of the above.
6. *Height 400 cm*. Catastrophic event with irreversible impacts.

2.4 Data analysis

We classified the maximum flow rates considering the “EN” (+) and “LN” (–) events. For example, ENSO |0.8 to 1| Weak (1), instead of 0.5 to 1, as suggested for the RdIP [21], |1 to 1.5| Moderate (2), |1.5 to 2| Strong (3) and | ≥ 2 | Very strong (4).

Furthermore, for the ONI criterion (quarterly), we applied the value of the last quarter October–November–December [O-N-D] and the quarter November–December–January [N-D-J] for the following year, except for 2009, which had a maximum in December, and the ONI of the O-N-D quarter was applied. When “EN” and “LN” coexist in the same year, the former was favoured; however, 1988 and 2006 were the two exceptions.

To describe the extreme data, we used the statistical program R (version 3.6.2), based on the Fisher-Tippett-Gnedenko theorem (FTG theorem), and we adjusted the data to a maximal distribution [37, 38]. Firstly, we adjusted the data to a generalised extreme value (GEV) distribution (Eq. 1) [modified from 39], using the L-moments method (LM) [39, 40]. Eq. (1) is the FTG theorem where μ is the location parameter,

and E is the scale parameter. The last one allows us to determine the extremal distribution. If $E < 0$, it is a Wumbell, $E > 0$, a Frechet and $E = 0$, a Gumbel [38]. Furthermore, the “Fitdistrplus” package helped determine the fit of the data to the extremal distribution determined by the E parameter [41].

In the statistical program R (version 3.6.2), based on the Fisher-Tippett-Gnedenko theorem (FTG theorem), we adjusted the data to a maximal distribution [37, 38]. Firstly, we adjusted the data to a GEV (Eq. 1) [modified from 39], using the L-moments method (LM) [39, 40]. Eq. (1) is the FTG theorem where μ is the location parameter, and E is the scale parameter. The last one allows us to determine the extremal distribution. If $E < 0$, it is a Wumbell, $E > 0$, a Frechet and $E = 0$, a Gumbel [38]. Furthermore, the “Fitdistrplus” package helped determine the fit of the data to the extremal distribution determined by the E parameter [41].

$$F(x) = \begin{cases} e^{-\left[1 + E\left(\frac{x - \mu}{\sigma}\right)\right]^{\frac{1}{E}}}, & E \neq 0 \\ e^{-e[-x]}, & E = 0 \end{cases} \quad (1)$$

In the study of extreme events, the “Values and Return Times” are defined as the values that will occur in a specific unit of time. On the other hand, the return time is the time that will elapse before a specific extreme value occurs. Therefore, frequency histograms were performed with the “ggplot2” packets to observe the behaviour of the data.

We used the parameters of partial η^2 and the F statistic to measure the strength of the relationship between the phenomena and the variance explained by the model.

Return times were calculated with the “extRemes” package [38, 42]. In addition, we performed Monte Carlo simulations, for which 50 random values of the extremal function were taken (representing the maximum values of 50 years), and the maximum value of the simulation was extracted, repeating 50,000 times. Finally, the probabilities of different extreme events occurring in the next 50 years were calculated based on the simulation.

3. Observed weather, climate and water-/sea-level trends and extremes

3.1 Weather and climate

3.1.1 Air temperature

Figure 2 shows the annual mean temperatures for Colonia, Carrasco and Rocha weather stations for 1989–2019. The three sites showed increasing trends close to 0.5°C . The annual maxima coincided in 2017 at Colonia and Carrasco, in 2002 at Rocha and the second maxima in Carrasco and Colonia.

3.1.2 Winds

The gusts of the winds at Carrasco weather station reached a maximum of 140.6 km/h due to an extreme extra-tropical cyclone in August 2005. Nevertheless,

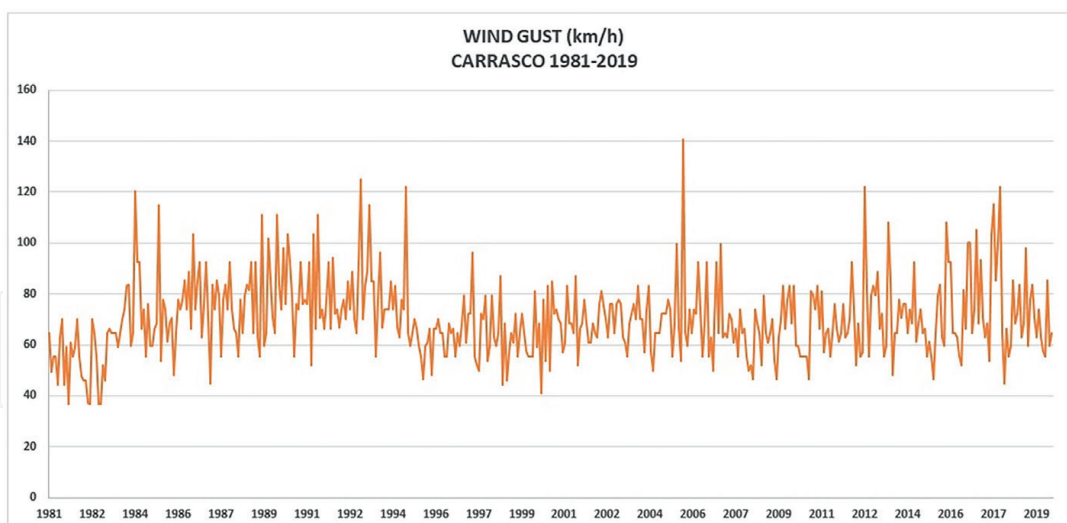


Figure 2. Evolution of annual mean temperatures ($^{\circ}\text{C}$) at Colonia, Carrasco and Rocha weather stations from 1980 to 2019.

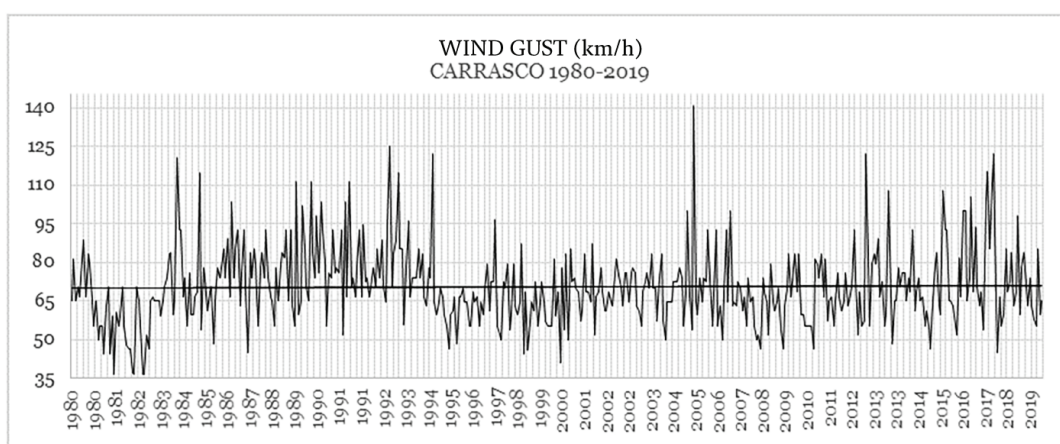


Figure 3. Monthly gusts of wind in Carrasco weather station (1981–2019).

maxima were not associated with ENSO events. **Figure 3** shows the gusts of winds in the Carrasco weather station (1980–2019) monthly. A slightly increasing trend from 65 to 67 $\text{km}\cdot\text{h}^{-1}$ is related to an increase in the minima.

Simulations with Monte Carlo show an occurrence probability of 99.8% for high-impact winds exceeding 129 $\text{km}\cdot\text{h}^{-1}$ over the next 50 years, with a return time of 29 years, while the acute winds of 140 $\text{km}\cdot\text{h}^{-1}$ have a probability of occurrence of 80% and a return time of 48 years.

3.2 ENSO and hydroclimatology

3.2.1 ONI index

Figure 4 shows the evolution of the ONI index from 1980 to 2019. The number of ENSO events was 21, with 11 “EN” events and 10 “LN” events. The former included weak to very strong events, whereas the latter included weak to strong ones. In addition, several events were pluriannual, accounted as an event.

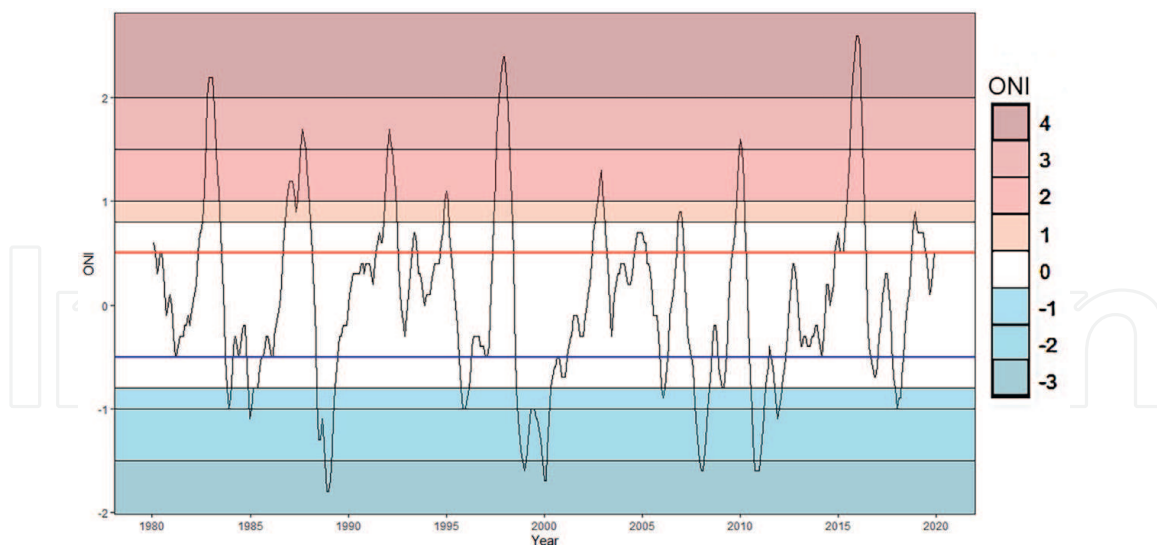


Figure 4.
 Evolution of the Ocean Niño Index (ONI) from 1980 to 2019. Above the red line: El Niño. Below the blue line: La Niña. Colours indicate the intensity of the ONI index according to our criteria (see section 2.4). Source: NOAA https://origin.cpc.ncep.noaa.gov/products/analysis_monitoring/ensostuff/ONI_v5.php

3.2.2 Rainfall and river flow

The annual mean precipitation in LPB showed a decreasing trend from 1980 to 2019 due to a change by 2002, with a minimum for 2019 that coincided with a “LN” (Figure 5). For instance, the time series 1975–2015 (not shown here) showed a positive trend due to the wet period until 1998–2002.

Figure 6 shows the accumulated yearly rainfall anomaly (mm) in 2008 (“LN”) (6a) and 2019 (“EN”) (6b).

Figure 7 shows the yearly Q_F (1980–2019, below) with an overall decreasing trend due to the lower inflows from 2003 to 2009 and 2018 to 2019, coinciding with “LN” and in the maxima coinciding with extreme “EN” events (1983, 1998, 2016). However, the Q_U (above) showed some degree of decoupling with the Q_F , with a sustained increase approaching $7000 \text{ m}^3\text{s}^{-1}$. Indeed, from 2014 to 2018, the discharges were close to 8,000 and 9,000 m^3s^{-1} , well above its average.

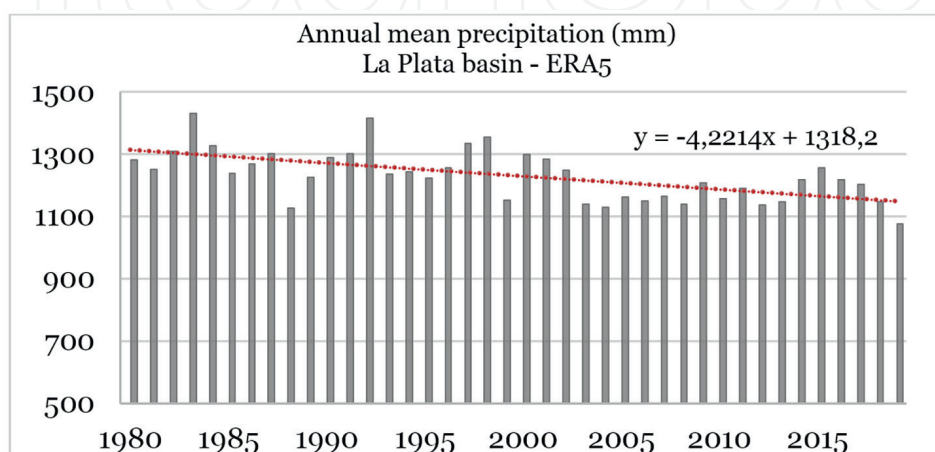


Figure 5.
 Annual mean precipitation (mm) over the La Plata basin (1980–2019) (The authors).

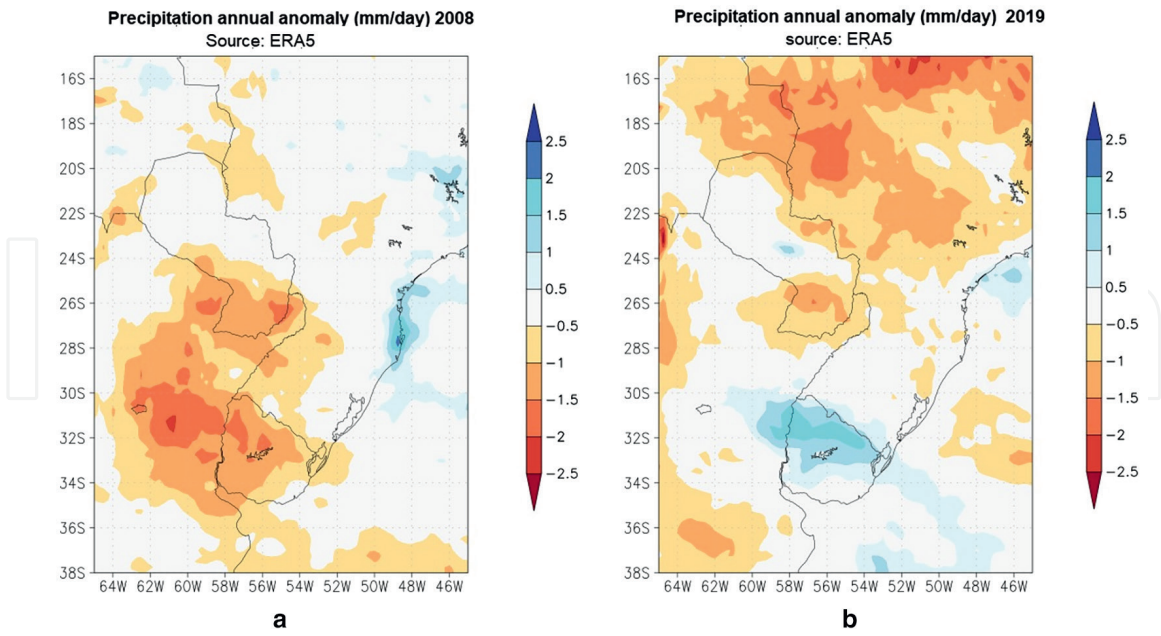


Figure 6. Accumulated rainfall anomaly (mm) from January to December 2008 (*La Niña*, a) and 2019 (*El Niño*, b) in *La Plata Basin* coinciding with ENSO events (The authors).

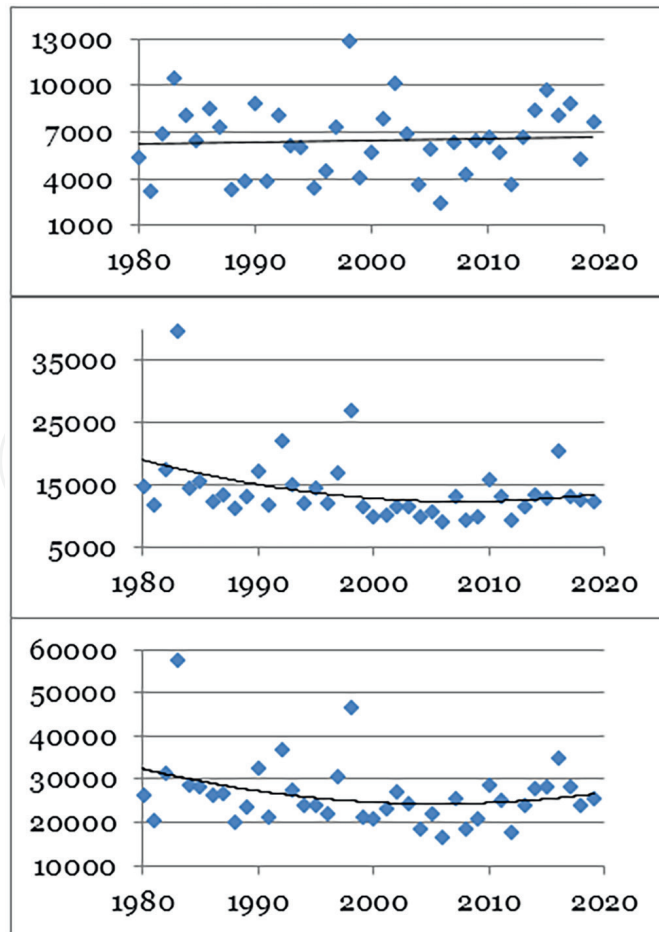


Figure 7. Total yearly river inflow (m^3s^{-1}), (Q_{Lb} above; Q_G , middle; Q_B below) from 1980 to 2019.

3.2.3 Extreme flows (EFs)

The Q_F (1980–2019) had maximum flows (EFs) ranging from $21,705 \text{ m}^3 \cdot \text{s}^{-1}$ to $88,349 \text{ m}^3 \cdot \text{s}^{-1}$ in 2006 and 1983, respectively. The EFs coincided with the maxima “EN” event recorded (1982–1983) and the maxima of the Paraná River, particularly, but not with that of the Q_U that presented the maximum during 2016. On the other hand, 2005–2006 coincided with a “LN”, which would explain the minimum flow value. As a result, the average Q_F during the study period was $42,428 \text{ m}^3 \cdot \text{s}^{-1}$, and the median was $38,227 \text{ m}^3 \cdot \text{s}^{-1}$ (**Figure 8**).

The yearly Q_F lower than the median includes cold or neutral years. Warm, cold and neutral ENSO events were identified above the median, although “EN” events predominated (**Figure 9**).

According to linear regression models, the maximum flow rates during the very strong “EN” (4) differed significantly from all other ENSO levels. The strong “EN” (3) differed from neutral and minor values (0 to –3). In contrast, the moderate and minor values had no significant differences (**Figure 9**, letters over boxplots). Despite this, the averages (black diamonds) and the medians show other non-significant

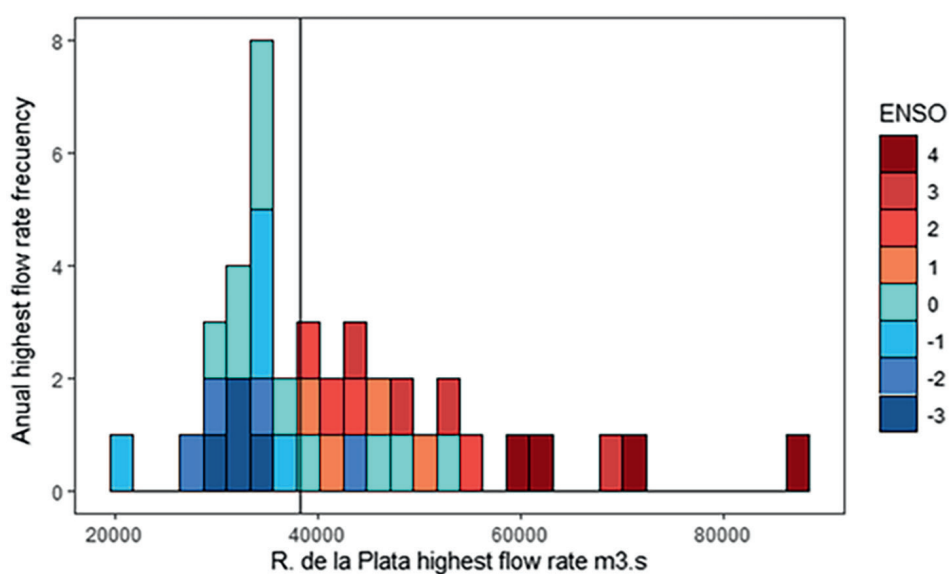


Figure 8.
 Histogram of the maximum flows ($\text{m}^3 \cdot \text{s}^{-1}$) of the Río de la Plata (1980–2019).

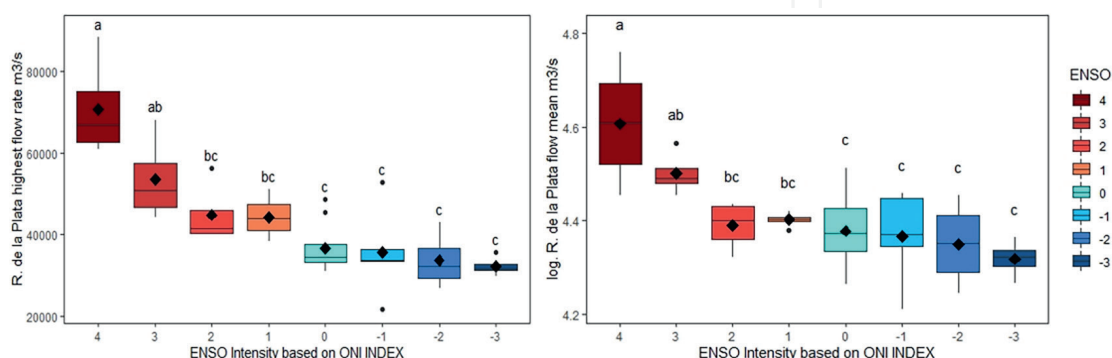


Figure 9.
 Left. Boxplot of maximum flows depending on the intensity of the ENSO. Right. Log in base 10 of the average flows ($\text{m}^3 \cdot \text{s}^{-1}$) depending on the intensity of the ENSO.

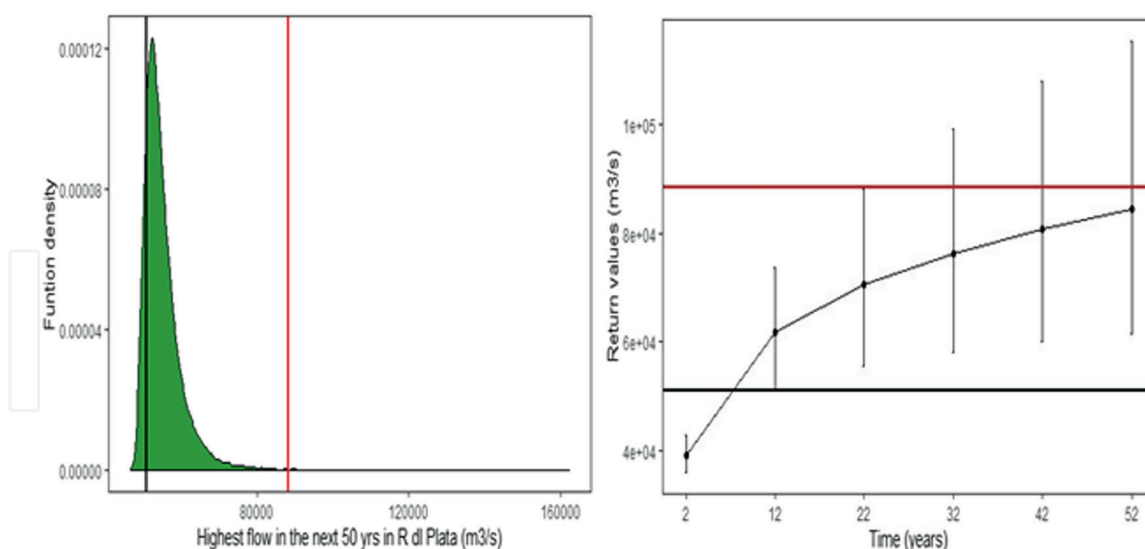


Figure 10.

Monte Carlo simulation of the maximum flows of the Río de la Plata at 50 years (left). 50-year return values. The historical maximum recorded is the black line ($51,670 \text{ m}^3 \cdot \text{s}^{-1}$, flow of 2019) and red line ($88,349 \text{ m}^3 \cdot \text{s}^{-1}$, right).

trends. According to measures of central tendency, moderate and strong “LN” appear to cluster (ONI: -3 and -2), as well as neutral years and weak “LN” (ONI: -1 and 0). We did the same analysis with the means, but only the “EN” $+3$ and $+4$ could be differentiated from the others. Regarding the extreme maximum flows (EQs) daily, **Figure 10 (left)** shows the function density of expected maxima (m^3/s).

The maxima model had a greater effect size (partial $\eta^2 = 0.71$ and $F(7.32) = 11.34$) than the mean model (partial $\eta^2 = 0.57$ and $F(7.32) = 6.16$). Consequently, for the flows, the levels assigned by the ONI index (neutral, weak, moderate, strong) could be revised because no differences were found between the categories.

Also, the effect of ENSO is more marked on maximum flows (EQs) than on averages. Based on historical records, the extreme flow recorded in 2019 would not have been so strange, occurring between 5 and 6 years (see return time, **Figure 10 right**, black line). The probability of observing in 50 years a maximum flow more remarkable than that observed during 2019 ($51,670 \text{ m}^3 \cdot \text{s}^{-1}$) is 83.95% (**Figure 10**). According to the Monte Carlo simulation, the probability of observing a flow more remarkable than that recorded in 1983 is 0.002. At the same time, the return values predict that this value would only occur once every 50 years (see **Figure 10 right**).

3.2.4 Extreme levels (ELs) at Montevideo

The extreme yearly levels (ELs) at Montevideo presented (1902–2021) (**Figure 11**) maximums ranging between 196 cm (2001) and 430 cm (1923). The average was 270 cm, and the highest levels were associated with ENSO events. The slight decreasing trend (red line) is because all the ELs > 320 cm occurred from 1914 to 1932, although ELs > 300 are again increasing over the last 40 years (1982–2021), as shown by the polynomial trend (blue line) and in **Table 2**.

Regarding the extreme levels (ELs) daily (**Figure 12 left**), the heights above the current maxima of 320 cm (since 1932) would be reached every 27 years, while the 350 cm height would occur every 52 years. Nevertheless, from 1980 to 2019, return values reaching the catastrophic ≥ 400 cm level are not expected. In the last 40 years, no clear pattern of cause-effect relationships was identified between ENSO events and ELs. Additionally,

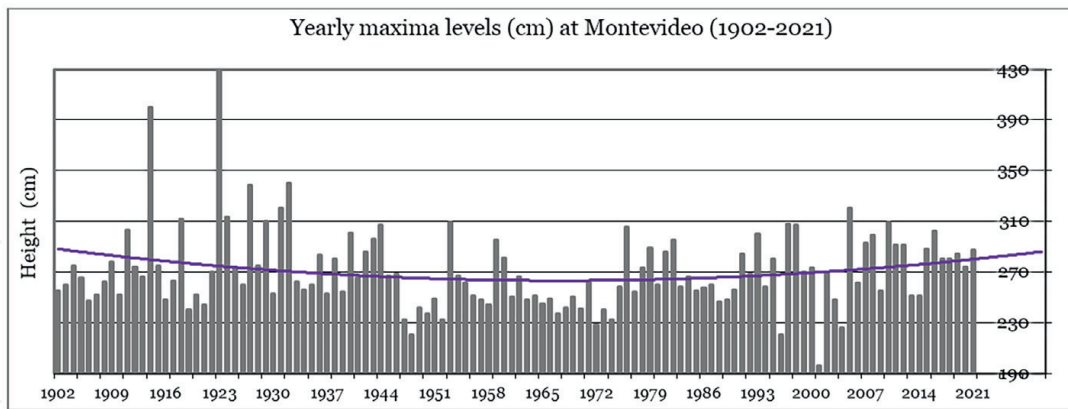


Figure 11.
 Extreme yearly levels (ELs) at Montevideo from 1902 to 2021.

Decade	Nb of events ≥ 200 cm	Nb of events ≥ 250 cm	Nb of events ≥ 280 cm
1983–1992	115	13	1
1993–2002	104	19	6
2003–2012	137	21	10
2013–2022	162	21	6

Table 2.
 The number of storm surges, by decade, from 1983 to 2022. It was updated until October 2022 from [10].

the extremal function behaved like a Weibull-type distribution, resulting from the maximal of a bounded function (such as the maxima of a uniform distribution), implying that in the last 40 years, the ELs were probably limited at their maximum (thus conditioning the predictions by both Monte Carlo simulations and return reset values).

However, in the last 120 years, some values departed from that bounded function, contributing to a light tail (**Figure 12** right), resembling a Gumbel-type distribution, which is the result of a light tail function (like the maxima of a normal one).

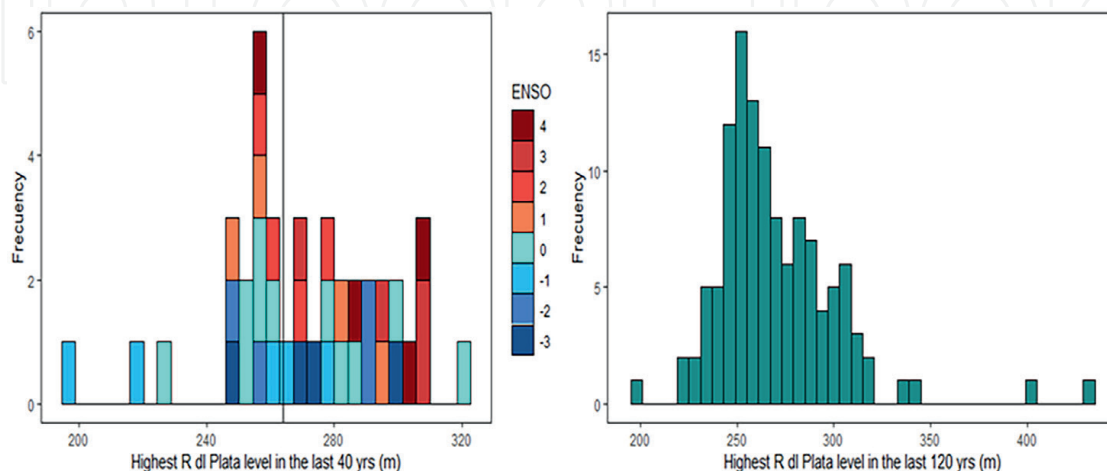


Figure 12.
 Histograms of the maximum levels (m) of the Río de la Plata in the last 40 years (colour according to the intensity of the ENSO), and the black line indicates the average (left) and last 120 years (right).

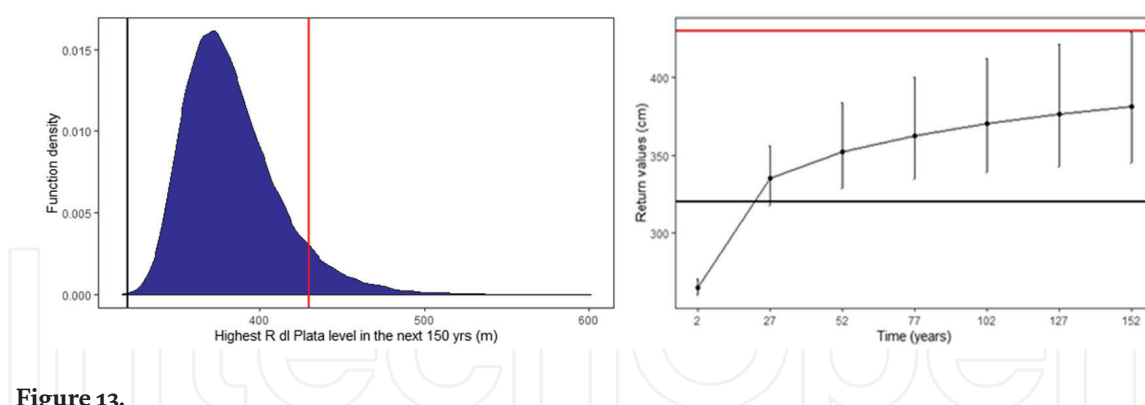


Figure 13. A. Density of results according to Monte Carlo models. B. Return values as a function of 150 years, with a 95% confidence interval. Black line: 320 cm, red line: 430 cm.

The probability of heights greater than 320 cm in 150 years is close to 100% according to the Monte Carlo simulation, while for the return times, these levels would occur every ten years (**Figure 13**). Therefore, it is highly likely that in 150 years, values of levels higher than those observed in the last 40 years will occur. The probability of witnessing another event like the one observed in 1923 (height: 430 cm) is improbable according to return times (see **Figure 13** left) because the values do not fall within the 95% confidence interval. However, in the simulations, a probability of 0.07 of having 430 cm or more values in the next 150 years was obtained (see **Figure 13** right). Quartiles 95 and 99 would be 438 and 478 cm, respectively, while the maximum would be 600 cm.

3.2.5 Occurrence of heights ≥ 200 cm (storm surges)

Table 2 shows the occurrence (decades) of storm surges at Montevideo from 1983 to 2022. Notably, the events ≥ 200 cm increased by 38% from 1983 to 2002 to 2003 to 2022.

3.3 Water-/sea-level time series

The water level at Colonia from 1981 to 2019 (**Figure 14** above) in the tidal river estuary (see **Figure 1**) showed an increase of 8 cm at a rate of 2.0 mm.yr^{-1} , accelerated since 1990.

The sea level at Montevideo from 1980 to 2019 (**Figure 14** middle) shows an increasing trend of 2.5 cm (0.6 mm.yr^{-1}), below the global trend, notably since 1990, accelerated since 2014. This low rate is partly explained by the very high level of 1981, the second highest ever (since 1902), after the maxima of 1998. However, since 2015, the levels have been within the range of 107–111 cm, 16–20 cm above the reference level (91 cm established in 1949) before the rise in MSL.

The sea level at Punta del Este from 1980 to 2019 (**Figure 14** below) increased by 11.5 cm (2.9 mm.yr^{-1}), with a sustained increase since 2014. Nevertheless, this time series is discontinuous due to the need for more data yearly over two short periods.

The compared water-/sea-level rise for the period 1954–2019 at Colonia and Montevideo and 1964–2019 at Punta del Este (**Figure 15**) showed an increase of 10.5 cm at Colonia (1.38 mm.yr^{-1}), 9.5 cm at Montevideo (1.25 mm.yr^{-1}) and 22 cm at Punta del Este (3.9 mm.yr^{-1}).

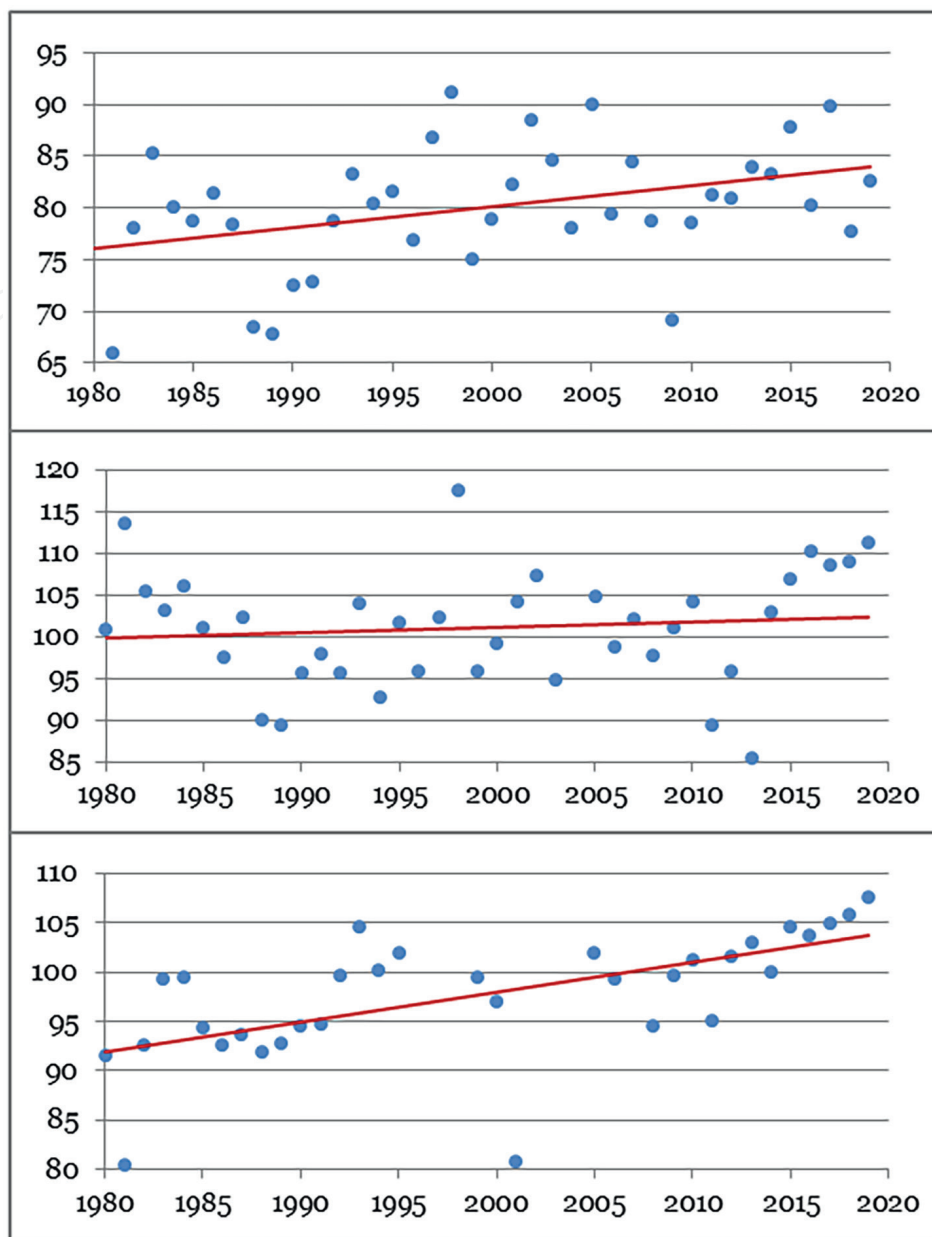


Figure 14. Water/sea level (cm) in Colonia (above), Montevideo (middle) and Punta del Este (below) (1980–2019).

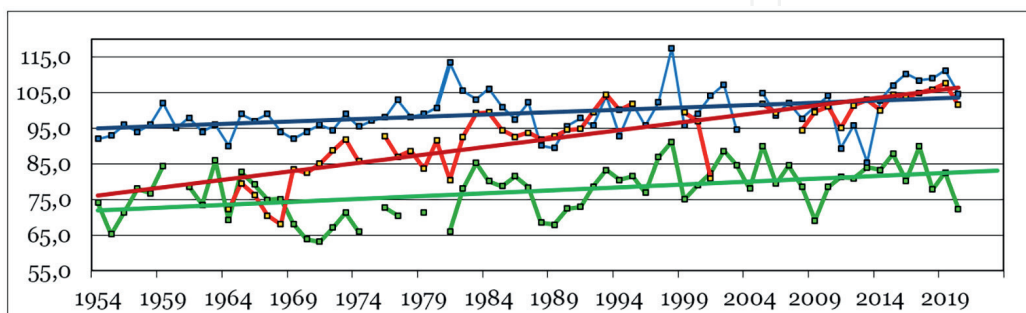


Figure 15. Water-/sea-level rise (cm) at Colonia (green below, 1954–2019), Montevideo (blue above, 1954–2019) and Punta del Este (red middle, 1964–2019) for the period 1954–2019.

4. Adaptation framework

Climate change and variability harm the coast, exposing infrastructure, residents and their means of livelihood, ecosystems and services to extreme events and sea-level rise (SLR) [43]. As a result, the Uruguayan Environment Ministry's Division of Climate Change (DCC) conducted a risk assessment and developed strategic lines on adaptation, ready to be executed in the short and long term [43, 44] as follows:

1. Strengthening the capacities to reduce climate change risk through early-warning systems.
2. Elaboration of Climate Change Coastal Adaptation Agendas at the municipality level.
3. Creation of knowledge regarding climate change and variability and technology transfer for coastal adaptation focused on vulnerability, SLR, extreme events, impact thresholds and coastal forms.
4. Encouragement of sustainable and climate change-resilient tourism.

Uruguay developed a National Adaptation Plan-Coasts (NAP-C) [43, 44] to implement the strategic action lines and consolidate platforms for sharing knowledge and information concerning adaptation at all governance levels and secure academic and civil society networks.

On the sub-national level, common priorities are managing the beach profile and dune ridges, recovering public coastal space and adapting spaces exposed to coastal floods [43]. In addition, municipalities address coastal erosion through "grey" or "green" solutions. For instance, from 2015 to 2020, alternative ecosystem-based solutions were developed [27, 45].

The NAP-C developed the following strategic lines of action on coastal adaptation. [43, 44]:

- *Deepening of knowledge and search for technological solutions about coastal processes and vulnerability to SLR and extreme events*
- *Coastal spatial planning*
- *Climate-resilient tourism strategies*
- *Restoration and recovery of dune systems, rain drainage management, beach accessibility and eroded areas*

The NAP-C also developed climate projections [44, 46, 47], aligned with the previous assessments based on the Representative Concentration Pathways (RCPs) for Uruguay [17, 26] and the observed trends.

- A quasi-linear rise in mean annual temperature
- A gradually increasing occurrence of extreme events associated with ENSO

According to another report of the CNAP [48], some climate-related risks and impacts (with medium to high certainty) based on the RCP scenarios (intermediate 4.5 and pessimistic 8.5) are as follows:

- A mean SLR of 80 cm (RCP8.5) by the end of the 21st century
- An increase of 43% in flood hazard by the end of the 21st century
- Significant damage to residential assets
- An increased ecosystem risk due to flood impact
- An increased beach erosion by 2050 (RCP4.5) due to the reduction of the protection service provided by the sand dynamics to arc-shaped beaches
- Damage caused by structural erosion due to SLR might exceed the annual erosion caused by extreme events by the end of the 21st century
- Significant effects on beaches due to the modification of flood levels and the retreat/advance of the shoreline. For a 2050 time horizon (RCP8.5), the shoreline of all Uruguayan beaches will retreat ≤ 5 m.

5. Discussion

This section discusses the Reasons for Concern (RFC) due to the observed weather, climate and water–/sea-level trends and extremes in the Rio de la Plata estuary (RdIP) and the research questions (RQs). The RFC show that only one metric can capture some of the dimensions of climate risk and the diversity of its consequences [9, 49]. First, we introduce how climate change, variability and extremes affect transitional and coastal areas in the context of the nine planetary boundaries [50, 51].

5.1 Reasons for concern (RFC) in transitional systems

The complex forces of climate change affect biogeochemical cycles, acidification and dissolved oxygen and nutrient levels in transitional and coastal areas [52], which are among the nine planetary boundaries [50, 51]. The ability of different coastal ecosystems (seagrass, marshes and estuaries) to cope with the effects of climate change is variable, as their vulnerabilities depend on local conditions [53].

Likewise, the change in the frequency and intensity of rainfall, SLR and increased climate variability, combined with greater urbanisation, more dams and agricultural intensification, will exacerbate the current problems in estuaries and coastal waters, affecting their resilience and resistance to natural hazards [52]. Additional limits, such as the biophysical processes, impose the need for further investigations, given the fundamental dependence of the global biosphere on ocean components and processes of marine and coastal systems. The challenge is to understand global changes and their consequences, for reducing the risk of crossing thresholds that lead to devastating and irreversible environmental changes while ensuring the maintenance of ecosystem services [54].

5.2 RFC in the RdIP

There are several increasing Reasons for Concern (RFC) in the RdIP associated with SLR, warming, the ENSO-related climate variability trends and the increasing occurrence of extreme river flows and water/sea height. We analyse the extreme weather events (RFC2), focusing on cyanobacterial blooms (Cyano-HABs) and beach erosion.

5.2.1 Global temperature and sea-level rise at the Rio de la Plata

According to Copernicus Global Climate Highlights 2022 [55], 2015–2022 was the warmest globally (maximum in 2016). However, by 2022, in some regions, such as the Uruguayan coast, influenced by the triennial La Niña event (2019–2022), there were slight negative anomalies relative to the 1991–2020 baseline, which are in line with the observed trends reported in previous studies [17, 19, 21, 22] and this chapter until 2019 (see **Figures 2, 5-7, 14**). Such observations highlight the importance of ENSO in the temperature, rainfall, river flow and wind regime variations and their effects on salinity, beach erosion and eutrophication processes in the RdIP and the Uruguayan coast.

On inter-annual timescales, the global mean sea level record shows significant variations related mainly to ENSO events [56], for instance, a rapid increase in sea level during EN-2015, followed by little change during 2016.

The water-/sea-level trend in the RdIP shows a maximum in 2016 (CL and MVD) and a minimum in 2009 (CL) and 2013 (MVD), linked to LN and EL events (see **Figures 14 and 15**). Nevertheless, these inner and middle estuary trends remain below the global trend. On the contrary, the recent SLR in Punta del Este on the border of the Atlantic Ocean, which is less river-influenced, with the accelerated rate since 2016, reaching maxima in 2018–2019, is more aligned with the global SLR trend, with more significant acceleration.

5.2.2 Extreme events and sea-level rise

Extreme weather events such as wind storms and extreme flow levels (ELs) can cause or trigger storm surges and sea floods, impacting the natural systems and built environment. In addition, these extremes may lead to a short-term linked sequence of events affecting vulnerable low-lying flood-prone coasts, which often persist after the storm diminishes [21, 22, 57, 58].

Severe and extreme “EN” have a more marked influence on the maxima flows and levels (EQs) and, to a less degree, on the extreme levels (ELs) than on averages (see **Figures 7-9**), thus causing more adverse impacts than a continuous effect caused by a slow-onset increasing trend in flow, height or wind. Furthermore, the implications of these extremes intensify the impacts due to coastal mismanagement, which can cause them to lose resilience [19, 33, 34].

In micro-tidal river-influenced environments like the RdIP, river flow forces the water/sea level variations seaward of the inner estuary [21, 22, 26]. Consequently, several authors have estimated the contribution of EQs to the sea level based on specific events [22], comparison between average water/sea level with those associated with strong El Niño [21, 26] and regression analysis between stream flow and sea level [59]. The former found that river flow contributed to a 5 to 20 cm increase in the level, thus increasing the risk in case of coupled “EN” and EQs with ELs extremes in the short term (24–72 hrs). The latter [59] found a sea level increase at Montevideo

of $0.48 \pm 0.38 \text{ mm.yr.}^{-1}$ and $0.71 \pm 0.35 \text{ mm.yr.}^{-1}$ at Buenos Aires (tidal river, close to Colonia) accounted for river inflow.

5.2.3 Application of extreme value approach: Intercomparison examples

Monte Carlo simulations help determine extreme flow and precipitation events and relate them to ENSO, for example, in the western United States [60]. Increases in the frequency of extreme events were mainly observed during El Niño, while events of a near-average nature did not see their frequency change, similar to what we observed in this study. Additionally, the FTG theorem has been used to determine the frequency of extreme flows in rivers in Mexico, considering the flows that could cause cyclonic events [61]. However, the Peaks on Thresholds method has been more effective in predicting extreme flows in Austria; even so, this methodology is more methodologically complex [39]. To determine the sea level, non-stationary GEV models are being used, which include parameters such as the increase in surface temperature or sea level, which allows for better observe the changes of the time series over time [62] because due to the increase in the level of the coast (**Figure 15**), the levels in the simulations could be underestimated.

5.2.4 Research questions

The research questions related to the RFC2 (RQ 1: Is the increase in extreme weather events and their risks to the coast from river/sea flooding and sea level rise (SLR) reaching high-risk levels? RQ 2: Are the extreme sea heights (ELS) increasing/decreasing or fluctuating over time?) are answered below:

Since 1980, the RFC2 in the RdLP northern coast has been steadily augmenting due to the following:

1. The steady increase in QU, reaching averages $\geq 7.000 \text{ m}^3.\text{s}^{-1}$, can govern the hydrological processes over tides and moderate winds [29], leading to environmental changes from eutrophication to invasive species [20, 63, 64].
2. The increasing occurrence of wind-induced storm surges has accelerated over the last 20 years. The impacts of ELs > 350 cm from 1914 to 1932 on the coastal environments [19, 34] exemplify how these impacts would increase compared to the usual 300 cm observed since 1932.
3. SLR serves as a metric of climate-related hazards where the transition from undetectable to moderate risk started before 1986–2005 [10, 18], increasing the risk of flooding. The risk is judged to reach a moderate level at about 10 cm above the 1986–2005 level [10]. Although SLR is still moderate [17, 18], without an appreciable impact yet, the acceleration since 2014 at Montevideo and Punta del Este suggests that these increasing levels, particularly since 2016, could become an impact soon, under a scenario of compounded risks due to extreme storm surges and river flow producing extreme levels, as suggested by several authors [17–22] before this recent acceleration.

5.2.5 Harmful cyanobacteria (Cyano-HABs)

In the LPB, the increase in flows leads to freshwater displacement to the estuary and Atlantic Ocean [28, 29, 65]. Furthermore, the climatic effects of “El Niño” favour

the appearance of cyanobacteria; the bloom that occurred in 2019 was exceptional due to the increase in surface temperature in the LP and RdLP and an extremely high Q_U [66–68] associated with the very strong EN in 2018–2019 (see **Figures 4** and **7**) causing the largest cyanobacteria bloom (Cyano-Habs) ever recorded in 2019 affecting the RdLP and Atlantic Ocean coast [65, 66].

The above hydroclimatic condition is not infrequent in the long term. For example, it happened eight times that the Q_U maximums and the other flow sources coincided in summer when the most oversized Cyano-HABs occur in the Uruguay River and the inner estuary. However, on 6 of these occasions, at least one moderate “EN” event is recorded that year ($ONI > 0.8^\circ C$).

Despite the above, this massive bloom is evidence that cultural eutrophication is deteriorating aquatic systems, generating a loss of water quality. Therefore, phenomena that previously could have gone unnoticed are currently generating problems at the ecosystemic, health and economic levels, becoming a RFC 2 related to the planetary boundaries [50, 51].

5.2.6 Climate-induced beach erosion

In the short term, ENSO-related variability influences erosion processes under strong “LN” or consecutive moderate or even weak events and intense and persistent SW and SE winds [19] or, conversely, accretion associated with “EN”. Furthermore, during the El Niño-related recovery, milder meridional winds prevail over the south quadrant ones occurring during “LN” [19]. In turn, the North Atlantic Oscillation (NAO) manifests at the decadal level, with a maximum of wind energy in the 1920s, a minimum in the 1970s and an increase from then to the present, appearing to be a cycle of circa 80 years or more [19] (see **Figure 11**).

The erosion in the unstable estuarine beaches can exceed four linear metres of retreat per year in wide arcs [19, 33, 34], while in the middle estuary area, the estimated retreat of pocket beaches is 1.70 metres per cm of rising in the mean sea level (MSL). Besides, considering a water-level increase of 15 cm, the estimation of beach retreat attributable to MSL change is up to 25.5 metres [34].

The data shown in Section 4 (Adaptation framework) highlight the need to arrest coastal mismanagements to reduce the risks due to SLR and flood hazards over the near future, posing a severe risk to coastal assets and beaches [19, 34, 48], by 2050–2100 [48].

6. Summary and conclusion

6.1 Summary

This chapter highlighted the RFC associated with impacts and adaptation on managing climate risk and disaster risk reduction [69]. This study’s most relevant and new outcomes (mainly climatic and hydrological data analyses from 1980 to 2019) along the Uruguay RdLP coast are as follows.

- The annual mean air temperature increased by $\sim 0.5^\circ C$.
- The maximum monthly gusts of winds in Carrasco slightly increased with 32 extreme events (90–109 km/h), 13 high-impact (110–140 km/h) and one acute (>140 km/h) event.

- The accumulated rainfall in the LPB showed a decreasing trend, reversing previous periods with increasing trends since the 1970s.
- The yearly Q_F showed a decreasing trend, aligned with the Paraná rivers since the mid-2000s. However, the Q_U continued its positive trend reaching close to the threshold of $7000 \text{ m}^3/\text{s}$ since 2014.
- The extreme flow distribution shows that all the outliers from the central tendency coincide with the very strong and one strong “EN” for the highest ones ($\geq 56,000 \text{ m}^3/\text{s}$) and with a weak “LN” for the lowest one. Also, the limits of the central tendency are related to “EN” and “LN”, respectively. The flow rates show a decreasing curvilinear trend from the “EN” + 4 to “LN” – 3, showing a significant jump from 2 to 3 and mainly 4.
- The probability of observing in 50 years a maximum flow exceeding the maximum ($51,670 \text{ m}^3/\text{s}$) recorded in 2019 is 83.95%, with a return time of 5–6 years. Moderate relationships between the ONI index and maximum flows are more remarkable for the maxima than for the averages.
- The water–/sea-level rise has continued at the three studied stations, accelerating since 2015 at Montevideo and Punta del Este. The latter showed an increasing rate above the local and global trends.
- The extreme yearly levels (ELs) at Montevideo showed from 1902 to 2021 a slight linear decreasing trend with maxima from 1914 to 1932 and a slight increase over the last 40 years, affecting the calculation of return periods. For instance, heights above 320 cm (the maximum since 1932) would occur every 27 years, while 350 cm height is expected every 52 years. There is no clear pattern of cause-effect relationships between ENSO events and ELs. For instance, return values reaching the catastrophic ≥ 400 cm level are improbable from the 1980–2019 data. The return times for the height 320 cm (from the 1902–2021 data) is only ten years, while the return of the extreme level ever (430 cm, recorded in 1923) is improbable because the values do not fall within the 95% confidence interval. The occurrence of storm surges over the last 40 years (1982–2021) has increased by 38% since 2013.
- Based on the observed trends and EQ return periods, cyano-HABs will likely occur shortly.
- Coastal erosion, including sandy beaches and the adverse impacts on the built environment, will likely significantly increase by 2050–2100.

7. Conclusion

During 1980–2019, the LPB rainfall and Q_F slightly decreased. However, the Uruguay River flow continued increasing, along with the air temperature, winds and sea level along the Northern coast of the RdLP, accelerating over the last 10–20 years.

Therefore, the climate risks have increased on the shoreline, and the Reasons for Concern are transitioning from undetectable to moderate and from moderate to high-risk levels due to the compound risk associated with |SLR + “EN” + wind-induced

storm surges| causing coastal flooding. The high and accelerating SLR at Punta del Este is particularly relevant.

Acknowledgements

We thank UdelaR full-time researchers' aid.

IntechOpen

Author details

Gustavo J Nagy^{1*}, José E Verocai¹, Leandro Capurro¹, Mónica Gómez-Erache¹, Ofelia Gutiérrez¹, Daniel Panario¹, Ernesto Brugnoli¹, Agustina Brum¹, Mario Bidegain² and Isabel C. Olivares³


1 Faculty of Sciences, University of the Republic, Institute of Environmental Sciences, Montevideo, Uruguay

2 Independent Researcher, Former chief of Climatology at the Uruguayan Institute of Meteorology (Inumet), Montevideo, Uruguay

3 Faculty of Sciences, University of Los Andes, Institute of Ecological and Environmental Sciences, Mérida, Venezuela

*Address all correspondence to: gnagy@fcien.edu.uy

IntechOpen

© 2023 The Author(s). Licensee IntechOpen. This chapter is distributed under the terms of the Creative Commons Attribution License (<http://creativecommons.org/licenses/by/3.0>), which permits unrestricted use, distribution, and reproduction in any medium, provided the original work is properly cited. 

References

- [1] Pörtner HO, Roberts DC, Adams H, Adler C, Aldunce P, Ali E, et al. Climate change 2022: Impacts, adaptation and vulnerability. Netherlands: IPCC; 2022. p. 3675. Available from: <https://edepot.wur.nl/565644> [Accessed on November 15, 2022]
- [2] Nagy GJ, Krishnapillai M, Saroar M, Olivares-Aguilera IC. Editorial: Climate risks, resilience and adaptation in coastal systems. *Frontiers in Climate*. 2023;4(109):0777. DOI: 10.3389/fclim.2022.1090577
- [3] Biguino B, Haigh ID, Dias JM, Brito AC. Climate change in estuarine systems: Patterns and gaps using a meta-analysis approach. *Science of the Total Environment*. 2023;858(1):159742. DOI: 10.1016/j.scitotenv.2022.159742
- [4] EPA. Climate adaptation and estuaries. Climate change adaptation resource Center (ARC-X). United States Environmental Protection Agency. 2022. Available online: <https://www.epa.gov/arc-x/climate-adaptation-and-estuaries> [Accessed on November 10, 2022]
- [5] Glamore W, Rayner D, Miller B, Rahman P, Dieber M. Estuaries in a Changing Climate. Sydney, NSW, Australia: Water Research Laboratory, School of Civil and Environmental Engineering, University of New South Wales; 2016; conferencecoastalconference.com/2016/papers2016/
- [6] Leal Filho W, Nagy GJ, Martinho F, et al. Influences of climate change and variability on estuarine ecosystems: An impact study in selected European, south American and Asian countries. *International Journal of Environmental Research and Public Health*. 2022;19(1):585
- [7] O'Neill B, van Aalst M, Zaiton Ibrahim Z, Berrang Ford L, Bhadwal S, Buhaug H, et al. Key risks across sectors and regions. In: Pörtner HO, Roberts DC, Tignor M, Poloczanska ES, Mintenbeck K, Alegría A, et al. *Climate Change 2022: Impacts, Adaptation, and Vulnerability: Contribution of Working Group II to the Sixth Assessment Report of the Intergovernmental Panel on Climate Change*. Cambridge: Cambridge University Press; 2022. pp. 2411-2538
- [8] Cooley S, Schoeman D, Bopp L, Boyd P, Donner S, Ghebrehiwet DY, et al. Ocean and coastal ecosystems and their services, in climate change 2022: Impacts, adaptation, and vulnerability. In: Pörtner H-O, Roberts DC, Tignor M, Poloczanska ES, Mintenbeck K, Alegría A, et al., editors. *Contribution of Working Group II to the Sixth Assessment Report of the Intergovernmental Panel on Climate Change*. Cambridge, United Kingdom; New York, NY, USA: Cambridge University Press; 2022
- [9] IPCC. 2014 Summary for policymakers. In: Field CB et al., editors. *Climate change 2014: Impacts, adaptation, and vulnerability. Part A: Global and sectoral aspects. Contribution of working group II to the fifth assessment report of the intergovernmental panel on climate change*. Cambridge, United Kingdom and New York, NY, USA: Cambridge University Press; 2014. pp. 1-32
- [10] O'Neill BC, Oppenheimer M, Warren R, Hallegatte S, Kopp RE, Pörtner HO, et al. IPCC reasons for concern regarding climate change risks. *Nature Climate Change*. 2017;7(1):28-37
- [11] Ropelewski C, Halpert MS. Global and regional scale precipitation

- patterns associated with the El Niño/southern oscillation. *Monthly Weather Review*. 1987;**115**(8):1606-1626. DOI: 10.1175/1520-0493(1987)115<1606:GARS PP>2.0.CO;2
- [12] Díaz A, Studzinski C, Mechoso C. Relationships between precipitation anomalies in Uruguay and southern Brazil and sea surface temperature in the Pacific and Atlantic oceans. *Journal of Climate*. 1998;**11**:251-271
- [13] Barros V, Grimm A, Doyle M. Relationship between temperature and circulation in southeastern South America and its influence from El Niño and La Niña events. *Journal Meteorology of Society Japan*. 2002;**80**:23-32
- [14] Feidler P. Environmental change in the eastern tropical Pacific Ocean review of ENSO and decadal variability. *Marine Ecology Progress Series*. 2002;**244**:265-283
- [15] Zhou and Lau. Principal modes of interannual and decadal variability of summer rainfall over southern America. *International Journal of Climatology*. 2001;**21**:1623-1644
- [16] Caffera R, Berbery E. La Plata Basin Climatology. In: Barros V, Clarke R, Días P, editors. *Climate Change in the La Plata Basin*. Research Centre for Sea and Atmosphere; Buenos Aires: CIMA-CONICET/FCEN-UBA; 2006. pp. 16-34
- [17] Nagy G, Bidegain M, Verocai J. de los Santos B, Escenarios climáticos Futuros Sobre Uruguay. Basado en los Nuevos Escenarios Socioeconómicos RCP. Project Report PNUD URU/11/G31, ClimateChangeDivision. Montevideo, Uruguay: MVOTMA; 2016
- [18] Nagy G, Gutiérrez O, Brugnoli E, Verocai J, Gómez-Erache M, Villamizar A, et al. Climate vulnerability, impacts and adaptation in central and south American coastal areas. *Regional Studies in Marine Science*. 2019;**29**:100683. DOI: 10.1016/j.rsma.2019.100683
- [19] Gutiérrez O, Panario D, Nagy GJ, Montes C, Bidegain M. Climate teleconnections and indicators of coastal systems response. *Ocean and Coastal Management*. 2016;**122**:64-76. DOI: 10.1016/j.ocecoaman.2016.01.009
- [20] Brugnoli E, Verocai J, Muniz P, García-Rodríguez F. Chapter 2 Weather, Hydrological and Oceanographic Conditions of the Northern Coast of the Río de la Plata Estuary during ENSO 2009-2010. In: Froneman W, editor. *Estuary*. London, UK: IntechOpen; 2018:19-38. DOI: 10.5772/intechopen.71808
- [21] Nagy G, Muñoz N, Verocai J, Bidegain M, Seijo L. Adjusting to current climate threats and planning adaptation: The case of the Uruguayan coastal zone within the Rio de la Plata river estuary. *Journal of Integrated Coastal Zone Management*. 2014;**14**(4):553-568. DOI: 10.5894/rgci472
- [22] Verocai J, Bidegain M, Gómez-Erache M, Nagy G. Addressing climate extremes in coastal management: The case of the Uruguayan coast of the Rio de la Plata system from 1983-2013. *International Journal of Integration Coastal Zone Management*. 2015;**15**(1):91-107
- [23] Codignotto O, Dragani W, Martin P, Simionato C, Medina R, Alonso G. Wind-wave climate change and increasing erosion in the outer Río de la Plata. *Argentina Continental Shelf Research*. 2012;**38**(15):110-116
- [24] Bacino G, Dragani W, Codignotto J. Changes in wave climate and its impact

on the coastal erosion in Samborombón Bay, Río de la Plata estuary, Argentina. *Estuarine, Coastal and Shelf Science*. 2019;**219**:71-80

[25] Barros V, Menéndez A, Nagy G. El cambio climático en el Río de la Plata. In: *Project Assessments of Impacts and Adaptation to climate change (AIACC)*, Centro de Investigaciones del Mar y la Atmósfera - CIMA/CONICET. Buenos Aires, Argentina; 2005. p. 200

[26] Verocai J, Nagy G, Bidegain B. Sea-level trends along freshwater and seawater mixing in the Uruguayan Rio de la Plata estuary and Atlantic Ocean coast. *International Journal of Marine Science*. 2016;**6**(7):1-18

[27] Carro I, Seijo L, Nagy G, Lagos X, Gutiérrez O. Building capacity on ecosystem-based adaptation strategy to cope with extreme events and sea-level rise on the Uruguayan coast. *International Journal of Climate Change Strategies and Management*. 2018;**10**(4):504-522. DOI: 10.1108/IJCCSM-07-2017-0149

[28] Nagy G, Gómez-Erache M, López C, Perdomo A. Distribution patterns of nutrients and symptoms of eutrophication in the Rio de la Plata River estuary system. *Hydrobiologia*. 2002;**475**:125-139

[29] Nagy G, Severov D, Pshennikov-Severova V, Delos Santos M, Lagomarsino J, et al. Río de la Plata estuarine system: Relationship between river flow and frontal variability. *Advances in Space Research*. 2008;**41**:1876-1881

[30] López Laborde J, Nagy GJ. Hydrography and sediment transport characteristics of the Rio de la Plata. In: Perillo G, Pino M, Piccolo C, editors. *Estuaries of South America; Their Geomorphology and Dynamics*. Berlin: Springer-Verlag; 1999. pp. 137-159

[31] Guerrero R, Acha E, Framiñan M, Lasta C. Physical oceanography of the Río de la Plata estuary, Argentina. *Continental Shelf Research*. 1997;**17**(7):727-742

[32] Acha EM, Mianzán H, Guerrero R, Carreto J, Giberto D, et al. An overview of physical and ecological processes in the Rio de la Plata estuary. *Continental Shelf Research*. N. 2008;**28**(13):1579-1588

[33] Gutiérrez O, Panario D. Caracterización y dinámica de la costa uruguaya, una revisión. In: Muniz P, Conde D, Venturini N, Brugnoli E, editors. *Ciencias Marino-Costas en el Umbral del Siglo XXI, Desafíos en Latinoamérica y el Caribe*. México DF: Editorial AGT S.A; 2019. pp. 61-91

[34] Gutiérrez O, Panario D, Nagy GJ, Piñeiro G, Montes C. Long-term morphological evolution of urban pocket beaches in Montevideo (Uruguay): impacts of coastal interventions and links to climate forcing. *Journal of Integrated Coastal Zone Management*. 2015;**15**(4):467-484. DOI: 10.5894/rgci553

[35] Hersbach H, Bell B, Berrisford P, Hirahara S, Horányi A, Muñoz-Sabater J et al. Complete ERA5 from 1979: Fifth generation of ECMWF atmospheric reanalyses of the global climate. Copernicus Climate Change Service (C3S) Data Store (CDS). 2017 [Accessed November 3, 2022]

[36] Stephenson DB. Definition, diagnosis, and origin of extreme weather and climate events. In: Diaz HF, Murnane RJ, editors. *Climate Extremes and Society*. Cambridge, UK: Cambridge University Press; 2008. pp. 11-23

[37] De Haan L, Ferreira A. *Extreme Value Theory: An Introduction*. New York: Springer Science & Business Media; 2006

- [38] Coles S, Bawa J, Trenner L, Dorazio P. An Introduction to Statistical Modeling of Extreme Values. Vol. 208. London: Springer; 2001. p. 208
- [39] Bezak N, Brilly M, Šraj M. Comparison between the peaks-over-threshold method and the annual maximum method for flood frequency analysis. *Hydrological Sciences Journal*. 2014;**59**(5):959-977
- [40] Wang J, Lu F, Lin K, Xiao W, Song X, He Y. Comparison and evaluation of uncertainties in extreme flood estimations of the upper Yangtze River by the Delta and profile likelihood function methods. *Stochastic Environmental Research and Risk Assessment*. 2017;**31**(9):2281-2296
- [41] Delignette-Muller M, Dutang C. *Fitdistrplus: An R package for fitting distributions*. *Journal of Statistical Software*. 2015;**64**:1-34
- [42] Gilleland E, Katz R. *extRemes 2.0: An extreme value analysis package in R*. *Journal of Statistical Software*. 2016;**72**(8):1-39
- [43] Ministry of the Environment/ SNRCC National Adaptation Plan to Climate Change and Variability for the Coastal Zone in Uruguay (COASTAL NAP). Montevideo: Ministry of the Environment; 2021. p. 68. Available from: <https://unfccc.int/sites/default/files/resource/NAP-Coastal-Uruguay.pdf>
- [44] Gómez EM. Lessons Learnt and Risk Management Best Practices from a Local Community Perspective. Uruguay: Intergovernmental Oceanographic Commission of UNESCO (IOC-UNESCO) and Directorate-General for Maritime Affairs and Fisheries of the European Commission (DG MARE); 2021. p. 28
- [45] Fitton J, Addo K, Jayson-Quashigah P, Nagy G, Gutiérrez O, Panario D, et al. Challenges to Climate Change Adaptation in Coastal Small Towns: Examples from Ghana. Uruguay, Finland, Denmark, and Alaska: *Ocean and Coast Management*; 2021;**212**:105787(1-7). DOI: 10.1016/J.OCECOAMAN.2021.105787
- [46] Barreiro M, Arizmendi F and Trinchín R. Proyecciones del climasobre Uruguay. Producto realizado en el marco del Plan Nacional de Adaptación Costera y el Plan Nacional de Adaptación en Ciudades, Convenio MVOTMA – Facultad de Ciencias; 2019, 31. Financiado por los proyectos PNUD-URU/16/G 34 y AECID-ARAUCLIMA 2016.
- [47] Barreiro, M, Arizmendi F and Trinchín R. Variabilidad observada del clima en Uruguay. Producto realizado en el marco del Plan Nacional de Adaptación Costera y el Plan Nacional de Adaptación en Ciudades, Convenio MVOTMA – Facultad de Ciencias; 2019, 52. Financiado por los proyectos PNUD URU/18/002 y AECID-ARAUCLIMA 2016.
- [48] IH-CANTABRIA. Informe técnico sobre la metodología en el proyecto. Escala nacional. Desarrollo de herramientas tecnológicas para evaluar los impactos, vulnerabilidad y adaptación al cambio climático en la zona costera de Uruguay. Informe técnico sobre los resultados del Proyecto. Escala nacional. Producto realizado en el marco del Plan Nacional de Adaptación Costera, MVOTMA - CTCN – AECID, 150 pp. 2019
- [49] Hino M, Field C, Mach K. Managed retreat as a response to natural hazard risk. *Nature Climate Change*. 2017;**7**:364-370
- [50] Steffen W, Richardson K, Rockström J, Cornell SE, Fetzer I, Bennet E, et al. Planetary boundaries: Guiding human development on a changing planet. *Science*. 2015;**347**(6223):2015
- [51] Persson L, Carney A, Collins CD, Cornell S, de Wit C, et al. Outside the safe

- operating space of the planetary boundary for novel entities. *Environmental Science & Technology*. 2022;56:1510-1521
- [52] Elliott M, Day JW, Ramachandran R, Wolanski E. Chapter 1—A synthesis: what is the future for coasts, estuaries, deltas and other transitional habitats in 2050 and beyond? In: Wolanski E, Day JW, Elliott M, Ramachandran R, editors. *Coasts and Estuaries*. Amsterdam, Netherlands; Oxford, UK; Cambridge, USA: Elsevier; 2019. pp. 1-28
- [53] Pacifici M, Foden W, Visconti P, Watson J, Butchart S, Kovacs K, et al. Assessing species vulnerability to climate change. *Nature Climate Change*. 2015;5:215-224
- [54] Nash K, Cvitanovic C, Fulton E, Halpern B, Milner-Gulland E, Watson R, et al. Planetary boundaries for a blue planet. *Ecology and Evolution*. 2017;1:1625-1634
- [55] Copernicus. The 2022 annual climate summary. *Global Climate Highlights 2022*. European Commission, ECMWF; 2022. Available online: <https://climate.copernicus.eu/global-climate-highlights-2022> [Accessed on November 12, 2022]
- [56] Cazenave A, Dieng H-B, Meyssignac B, von Schuckmann K, Decharme B, Berthier E. The rate of sea-level rise. *Nature Climate Change*. 2014;4:358-361. DOI: 10.1038/nclimate2159
- [57] Moreno J, Laguna-Defior C, Barros V, Calvo Buendía E, Marengo J, Oswald U. *Adaptation to Climate Change Risks in Ibero-American Countries — RIOCCADAPT Report: 2020*. Madrid, Spain: McGraw-Hill;
- [58] Wang H, Li W, Xiang W. Sea level rise along China coast in the last 60 years. *Acta Oceanologica Sinica*. 2022;41(12):1-9
- [59] Piecuch C. River effects on sea-level rise in the Río de la Plata during the past century. *EGUsphere*. 2022;7:1-30
- [60] Cayan DR, Redmond KT, Riddle LG. ENSO and hydrologic extremes in the western United States. *Journal of Climate*. 1999;12(9):2881-2893
- [61] Molina-Aguilar JP, Gutierrez-Lopez A, Raynal-Villaseñor JA, Garcia-Valenzuela LG. Optimization of parameters in the generalized extreme-value distribution type 1 for three populations using harmonic search. *Atmosphere*. 2019;10(5):257
- [62] Wong TE, Sheets H, Torline T and Zhang M (2022) evidence for increasing frequency of extreme Coastal Sea levels. *Frontiers in Climate*. 2022;4:796479. DOI: 10.3389/fclim.2022.796479
- [63] Brugnoli E, Arocena R, Muniz P, Cabrera-Lamanna L. Management and monitoring of eutrophication: Trophic state indexes on the Río de la Plata northern coast. In: Leal Filho W, Azul AM, Brandli L, Lange Salvia A, Wall T, editors. *Life Below Water. Encyclopedia of the UN Sustainable Development Goals*. Cham: Springer; 2021
- [64] Brugnoli E, Pereira J, Clemente J, Muniz P and Capurro L. CAPÍTULO VIII. *Limnoperna fortunei* (Mejillón dorado): características bióticas, distribución, impactos y manejo poblacional en Uruguay - CEEI *Invasiones Biológicas*. In book: *Especies exóticas invasoras de Uruguay: distribución, impactos socioambientales y estrategias de gestión* Publisher: Retema-UdelaR/CEEI, Ministerio de Ambiente; 2022. Montevideo
- [65] Brugnoli E, Muniz P, Venturini N, Brena B, Rodríguez A, García-Rodríguez F. Assessing multimetric trophic state

variability during an ENSO event in a large estuary (Río de la Plata, South America). *Regional studies in marine. Science*. 2019;**28**:100565

[66] Kruk C, Martínez A, de la Martínez Escalera G, Trinchin R, Manta G, Segura A, et al. Floración excepcional de cianobacterias tóxicas en la costa de Uruguay, verano 2019. In: *INNOTEC*. 2021;**18**:36-68. DOI: 10.26461/18.06

[67] Aubriot L, Zabaleta B, Bordet F, Sienna D, Risso J, Achkar M, et al. Assessing the origin of a massive cyanobacterial bloom in the Río de la Plata (2019): Towards an early warning system. *WaterResearch*. 2020;**181**(15):115944. DOI: 10.1016/j.watres.2020.115944

[68] Goyenola G, Kruk C, Mazzeo N, Nario A, Perdomo C, Piccini C, et al. Producción, nutrientes, eutrofización y cianobacterias en Uruguay: armando el rompecabezas. In: *INNOTEC*. 2021;**22**:e558(1-33). DOI: 0.26461/22.02

[69] Patwardhan A, Downing T, Leary N, Wilbanks T. Towards an integrated agenda for adaptation research: Theory, practice and policy: Strategy paper. *Current Opinion in Environmental Sustainability*. 2009;**1**(2):219-225. DOI: 10.1016/j.cosust.2009.10.010